Kasetsart J. (Nat. Sci.) 43 : 822 - 832 (2009)

Calculation of Potential Flow Around an Oblate Spheroid Using Indirect Boundary Element Method

Muhammad Mushtaq*, Nawazish Ali Shah, Ghulam Muhammad and Gul-e-Zehra Rizve

ABSTRACT

An indirect boundary element method was applied to calculate a potential flow around an oblate spheroid. The computed results for flow velocities were compared with analytical results. The accuracy of the computed results was quite good.

Key words: boundary element method, potential flow, axisymmetric flow, oblate spheroid, planetary ellipsoid

INTRODUCTION

It has always been a struggle in fluid flow modeling to find more efficient numerical methods that can be used to solve a complicated system of partial differential equations (PDE) of fluid flows. The calculation of practical flows was made possible over time by the development of many numerical techniques, such as the finite difference method, the finite element method, the finite volume method and the boundary element method. These methods, which have evolved with the discovery of new algorithms and the availability of faster computers, are CPU time and storage hungry. One of the advantages of the boundary element method is that the entire surface of the body has to be discretized, whereas with domain methods it is essential to discretize the entire region of the flow field. The most important characteristics of the boundary element method are the much smaller system of equations and the considerable reduction in data, with the latter being a prerequisite to run a computer program efficiently. These methods have been successfully applied in a number of fields, including elasticity, potential theory, elastostatics and elastodynamics (Brebbia, 1978; Brebbia and Walker, 1980). Furthermore, this method is well suited to problems having an infinite domain. Thus, it is concluded that the boundary element method is a time-saving, accurate and efficient numerical technique compared with other numerical techniques. It can be classified into direct boundary element and indirect boundary element methods. The direct boundary element method has been used for flow field calculations around complicated bodies (Morino *et al*., 1975). The indirect method utilizes a distribution of singularities over the boundary of the body and computes this distribution as the solution of the integral equation. The indirect method has been used for many years for flow field calculations surrounding three-dimensional bodies (Hess and Smith, 1967; Hess, 1973).

Department of Mathematics, University of Engineering & Technology, Lahore – 54890 Pakistan.
* Corresponding author, e-mail: mushtaqmalik2004@yahoo.co.uk

Received date : 31/03/09 Accepted date : 19/06/09

Flow past an oblate spheroid

Let an oblate spheroid be generated by rotating an ellipse of semi-major axis a and semi-minor axis b about its minor axis and let a uniform stream of velocity U be in the positive direction of the z axis as shown in the Figure 1.

An axi-symmetric flow is most conveniently formulated using cylindrical polar coordinates. The cylindrical polar coordinates are taken as (r, θ, z).

In Shah (2008) the oblate spheroid is defined by the transformation:

$$\begin{aligned} z + i\,r &= c \sinh \zeta \\ &= c \sinh (\xi + i\,\eta) \\ &= c (\sinh \xi \cos \eta + i \cosh \xi \sin \eta) \\ &= c \sinh \xi \cos \eta + i\, c \cosh \xi \sin \eta \end{aligned}$$

Comparing real and imaginary parts, we have (Equation 1):

$$z = c \sinh \xi \cos \eta \quad r = c \cosh \xi \sin \eta \quad (1)$$

Therefore the curve $\xi = \xi_0$ is an ellipse in the z r plane whose semi-axes are (Equation 2):

$$a = c \cosh \xi_0 \quad b = c \sinh \xi_0 \quad (2)$$

and so $\xi = \xi_0$ is an oblate spheroid

The stream function ψ for an oblate spheroid moving in the negative direction of the z axis, with velocity U can be calculated as in Shah, 2008 (Equation 3):

$$\psi = \frac{\frac{1}{2} U c^2 \left[\sinh \xi - \cosh^2 \xi \cot^{-1}(\sinh \xi)\right] \sin^2 \eta}{e\sqrt{1-e^2} - \sin^{-1} e} \quad (3)$$

where e is the eccentricity.

The stream function ψ for the uniform stream with velocity U in the positive direction of the z axis is also given by Shah (2008) (Equation 4):

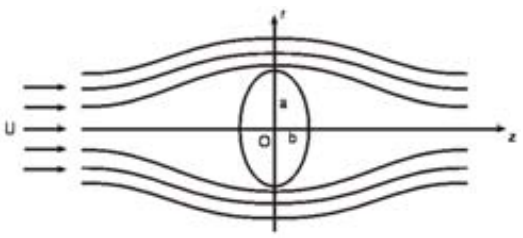

Figure 1 The flow past an Oblate spheroid.

$$\psi = -\frac{1}{2} U r^2 \quad (4)$$

Therefore, the stream function ψ for the streaming motion past a fixed oblate spheroid in the positive direction of the z axis becomes

$$\psi = -\frac{1}{2} U r^2 + \frac{-\frac{1}{2} U c^2 \left[\sinh \xi - \cosh^2 \xi \cot^{-1}(\sinh \xi)\right] \sin^2 \eta}{e\sqrt{1-e^2} - \sin^{-1} e}$$

which, on substituting from (1) becomes Equation 5:

$$\psi = -\frac{1}{2} U c^2 \cosh^2 \xi \sin^2 \eta + \frac{\frac{1}{2} U c^2 \left[\sinh \xi - \cosh^2 \xi \cot^{-1}(\sinh \xi)\right] \sin^2 \eta}{e\sqrt{1-e^2} - \sin^{-1} e} \quad (5)$$

To determine the formula for the velocity, the relation in Equation 6 is used (Milne-Thomson, 1968; Shah, 2008)

$$V^2 r^2 f'(\zeta)\, \overline{f}'(\zeta) = \left(\frac{\partial \psi}{\partial \xi}\right)^2 + \left(\frac{\partial \psi}{\partial \eta}\right)^2 \quad (6)$$

Since $f(\zeta) = c \sinh \zeta$, therefore

$f'(\zeta) = c \cosh \zeta = c \cosh (\xi + i\,\eta)$,

$\overline{f}'(\zeta) = c \cosh (\zeta - i\,\eta)$

and $f'(\zeta)\, \overline{f}'(\zeta) = c^2 (\cosh^2 \xi \cos^2 \eta + \sinh^2 \xi \sin^2 \eta)$ (7)

When $\xi = \xi_0$, then from (1) , (6) and (7)

$$V^2 c^4 \cosh^2 \xi_0 \sin^2 \eta \,(\cosh^2 \xi_0 \cos^2 \eta + \sinh^2 \xi_0 \sin^2 \eta) = \left(\frac{\partial \psi}{\partial \xi}\right)^2_{\xi=\xi_0} + \left(\frac{\partial \psi}{\partial \eta}\right)^2_{\xi=\xi_0} \quad (8)$$

Now from (5), we get

$$\left(\frac{\partial \psi}{\partial \xi}\right)_{\xi=\xi_0} = -U c^2 \cosh \xi_0 \sinh \xi_0 \sin^2 \eta + \frac{U c^2 \left[\cosh \xi_0 - \cosh \xi_0 \sinh \xi_0 \cot^{-1}(\sinh \xi_0)\right] \sin^2 \eta}{e\sqrt{1-e^2} - \sin^{-1} e} \quad (9)$$

Since for an oblate spheroid

$$a = c \cosh \xi_0 , \quad b = c \sinh \xi_0 \quad (10)$$

But $\cot^{-1}(\sinh \xi_0) = \theta$, $e = \sin \theta = \frac{c}{a}$

and $\sqrt{1-e^2} = \cos\theta = \frac{b}{a}$ (11)

From (9), (10), and (11), we get

$$\left(\frac{\partial\psi}{\partial\xi}\right)_{\xi=\xi_0} = U\sin^2\eta \left\{-ab + \frac{a\,c - a\,b\,\theta}{\frac{c}{a}\cdot\frac{b}{a} - \theta}\right\} =$$

$$U\sin^2\eta \left\{-ab + \frac{a\,c - a\,b\,\theta}{b\,c - a^2\,\theta}a^2\right\} \quad (12)$$

and from (5), (10) and (11), we obtain

$$\left(\frac{\partial\psi}{\partial\eta}\right)_{\xi=\xi_0} = 0 \quad (13)$$

Using (12) and (13), (8) becomes

$V^2 c^4 \cosh^2\xi_0 \sin^2\eta\,[\cosh^2\xi_0\cos^2\eta + \sinh^2 x_0 \sin^2\eta\,] = U^2\sin^4\eta$

$$\left[-a\,b + \frac{a\,c - a\,b\,\theta}{b\,c - a^2\,\theta}a^2\right] \quad (14)$$

But from (1) and (2), we get

$$\cos\eta = \frac{z}{b}, \quad \sin\eta = \frac{r}{a} \quad (15)$$

Using (10), (15) in (14), we have

$$V^2 = \frac{U^2\,r^2\,b^2\,c^6}{(b\,c - a^2\,\theta)^2\,(a^4 - z^2 + b^4 - r^2)^2} \quad (16)$$

where $\theta = \sin^{-1}\left(\frac{c}{a}\right)$

Taking the square root of (16), the magnitude of the exact velocity distribution over the boundary of an oblate spheroid is given by

$$V = \frac{U\,b\,c^3\,r}{(b\,c - a^2\,\theta)\sqrt{a^4\,z^2 + b^4\,r^2}}$$

Boundary conditions

The boundary condition to be satisfied over the surface of an oblate spheroid is shown in Equation 17:

$$\frac{\partial\phi_{o.s}}{\partial n} = U(\hat{n}\cdot\hat{k}) \quad (17)$$

where $\phi_{o.s}$ is the perturbation velocity potential of an oblate spheroid and $\hat{n}$ is the outward drawn unit normal to the surface of an oblate spheroid.

The equation of the boundary of the oblate spheroid $\frac{z^2}{b^2} + \frac{y^2}{a^2} + \frac{x^2}{a^2} = 1$

Let $f(x, y, z) = \frac{z^2}{b^2} + \frac{y^2}{a^2} + \frac{x^2}{a^2} - 1$

Then $\nabla f = \frac{2x}{a^2}\hat{i} + \frac{2y}{a^2}\hat{j} + \frac{2z}{b^2}\hat{k}$

$$\text{Therefore } \hat{n} = \frac{\nabla f}{|\nabla f|} = \frac{\frac{2x}{a^2}\hat{i} + \frac{2y}{a^2}\hat{j} + \frac{2z}{b^2}\hat{k}}{\sqrt{\left(\frac{2z}{b^2}\right)^2 + \left(\frac{2y}{a^2}\right)^2 + \left(\frac{2x}{a^2}\right)^2}}$$

$$\text{Thus } \hat{n}\cdot\hat{k} = \frac{\frac{2z}{b^2}}{\sqrt{\left(\frac{2z}{b^2}\right)^2 + \left(\frac{2y}{a^2}\right)^2 + \left(\frac{2x}{a^2}\right)^2}}$$

$$= \frac{\frac{z}{b^2}}{\sqrt{\frac{z^2}{b^4} + \frac{y^2}{a^4} + \frac{x^2}{a^4}}}$$

Therefore, the boundary condition in (17) takes the form

$$\frac{\partial\phi_{o.s}}{\partial n} = U\frac{\frac{z}{b^2}}{\frac{\sqrt{a^4\,z^2 + b^4\,y^2 + b^4\,x^2}}{a^2\,b^2}}$$

$$= \frac{z\,a^2}{\sqrt{a^4\,z^2 + b^4\,(y^2 + x^2)}}$$

(Taking U = 1) (18)

Equation 18 is the boundary condition, which must be satisfied over the boundary of an oblate spheroid.

DISCRETIZATION OF ELEMENTS

Consider the surface of the sphere in one octant to be divided into three quadrilateral elements by joining the centroid of the surface with

the mid points of the curves in the coordinate planes as shown in Figure 2 (Mushtaq *et al.*, 2009).

Then, each element is divided further into four elements by joining the centroid of that element with the midpoint of each side of the element. Thus one octant of the surface of the sphere is divided into 12 elements and the whole surface of the body is divided into 96 boundary elements and so on. The above-mentioned method is adopted in order to produce a uniform distribution of elements over the surface of the body.

Figure 3 shows the method for finding the coordinate (x_p, y_p, z_p) of any point P on the surface of the sphere.

Figure 3 provides the following equation

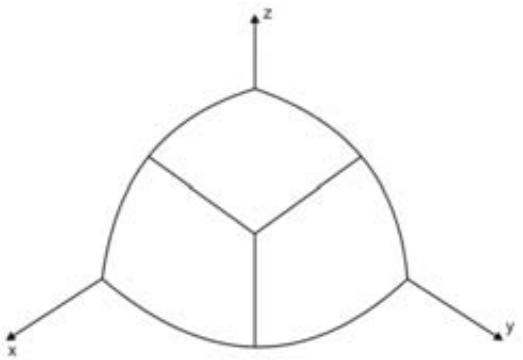

Figure 2 Surface of the sphere divided into three quadrilateral elements.

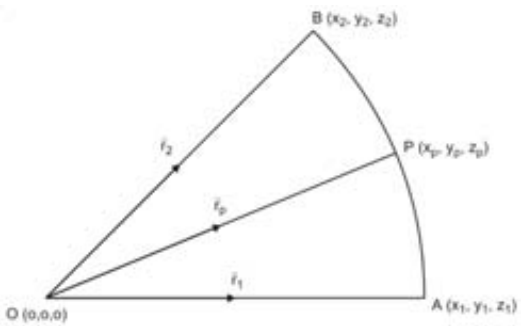

Figure 3 The method of finding the coordinate (x_p, y_p, z_p) of any point P on the surface of the sphere.

$$\left|\vec{r}_p\right| = 1$$

$$\vec{r}_p \cdot \vec{r}_1 = \vec{r}_p \cdot \vec{r}_2$$

$$\left(\vec{r}_1 \times \vec{r}_2\right) \cdot \vec{r}_p = 0$$

or in Cartesian form

$$x_p^2 + y_p^2 + z_p^2 = 1$$

$$x_p (x_1 - x_2) + y_p (y_1 - y_2) + z_p (z_1 - z_2) = 0$$

$$x_p (y_1 z_2 - z_1 y_2) + y_p (x_2 z_1 - x_1 z_2) + z_p (x_1 y_2 - x_2 y_1) = 0$$

As the body possesses planes of symmetry, this fact may be used in the input to the program and only the non–redundant portion needs to be specified by input points. The other portions are automatically taken into account. The planes of symmetry are taken to be the coordinate planes of the reference coordinate system. The advantage of the use of symmetry is that it reduces the order of the resulting system of equations and consequently reduces the computing time in running a program. As a sphere is symmetric with respect to all three coordinate planes of the reference coordinate system, only one eighth of the body surface need be specified by the input points, while the other seven eighths can be accounted for by symmetry.

The oblate spheroids of fineness ratios 2 and 10 were discretized into 24, 96 and 384 boundary elements and the computed velocity distributions compared with analytical solutions for the oblate spheroids. For both spheroids, the input points were distributed on the surface of a sphere and the x and y-coordinates of these points were then divided by the fineness ratios to generate the points for the oblate spheroids. The number of boundary elements used to obtain the computed velocity distribution was the same as that used for the sphere.

The calculated velocity distributions were compared with analytical solutions for the oblate spheroid of fineness ratios 2 and 10 using Fortran programming.

Figures 4, 6 and 8 show the comparison of the computed and analytical distributions over the surface of an oblate spheroid of fineness ratio 2 for 24, 96 and 384 boundary elements, respectively. Figures 5, 7 and 9 show the comparison of the computed and analytical distributions over the surface of an oblate spheroid of fineness ratio 10 for 24, 96 and 384 boundary elements, respectively. The accuracy of the calculated results in both case of an oblate spheroid of fineness ratio 2 and 10 is seen to be good.

Table 1 Comparison of the computed velocities with exact velocity over the surface of an oblate spheroid with fineness ratio 2 using 24 boundary elements.

Element	XM	YM	ZM	$R = \sqrt{(YM)^2 + (ZM)^2}$	Computed velocity	Exact velocity
1	-.161E+00	-.748E+00	.321E+00	.81391E+00	.14559E+01	.20456E+01
2	-.374E+00	-.321E+00	.321E+00	.45412E+00	.52484E+00	.75697E+00
3	-.374E+00	.321E+00	.321E+00	.45412E+00	.52484E+00	.75697E+00
4	-.161E+00	.748E+00	.321E+00	.81391E+00	.14559E+01	.20456E+01
5	.161E+00	.748E+00	.321E+00	.81391E+00	.14559E+01	.20456E+01
6	.374E+00	.321E+00	.321E+00	.45412E+00	.52484E+00	.75697E+00
7	.374E+00	-.321E+00	.321E+00	.45412E+00	.52484E+00	.75697E+00
8	.161E+00	-.748E+00	.321E+00	.81391E+00	.14559E+01	.20456E+01
9	-.161E+00	-.321E+00	.748E+00	.81391E+00	.14559E+01	.20456E+01
10	-.161E+00	.321E+00	.748E+00	.81391E+00	.14559E+01	.20456E+01
11	.161E+00	.321E+00	.748E+00	.81391E+00	.14559E+01	.20456E+01
12	.161E+00	-.321E+00	.748E+00	.81391E+00	.14559E+01	.20456E+01

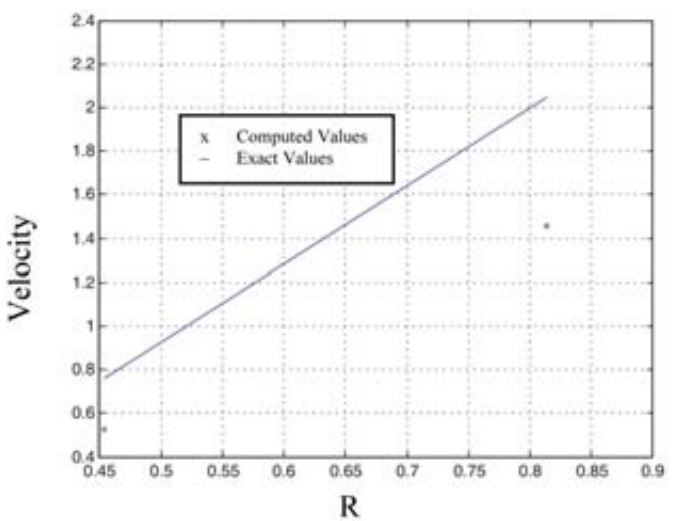

Figure 4 Comparison of computed and analytical velocity distributions over the surface of an oblate spheroid using 24 boundary elements with fineness ratio 2.

CONCLUSION

An indirect boundary element method was applied to calculate the incompressible potential flow around an oblate spheroid. The computed flow velocities obtained by this method were compared with the analytical solutions for flow past an oblate spheroid. It was found that the computed results for velocity distribution were in good agreement with the analytical results for the body under consideration.

Table 2 Comparison of the computed velocities with exact velocity over the surface of an oblate spheroid with fineness ratio 10 using 24 boundary elements.

Element	XM	YM	ZM	$R = \sqrt{(YM)^2 + (ZM)^2}$	Computed velocity	Exact velocity
1	-.321E-01	-.748E+00	.321E+00	.81391E+00	.15726E+01	.17673E+01
2	-.748E-01	-.321E+00	.321E+00	.45412E+00	.36626E+00	.43595E+00
3	-.748E-01	.321E+00	.321E+00	.45412E+00	.36626E+00	.43595E+00
4	-.321E-01	.748E+00	.321E+00	.81391E+00	.15726E+01	.17673E+01
5	.321E-01	.748E+00	.321E+00	.81391E+00	.15726E+01	.17673E+01
6	.748E-01	.321E+00	.321E+00	.45412E+00	.36626E+00	.43595E+00
7	.748E-01	-.321E+00	.321E+00	.45412E+00	.36626E+00	.43595E+00
8	.321E-01	-.748E+00	.321E+00	.81391E+00	.15726E+01	.17673E+01
9	-.321E-01	-.321E+00	.748E+00	.81391E+00	.15726E+01	.17673E+01
10	-.321E-01	.321E+00	.748E+00	.81391E+00	.15726E+01	.17673E+01
11	.321E-01	.321E+00	.748E+00	.81391E+00	.15726E+01	.17673E+01
12	.321E-01	-.321E+00	.748E+00	.81391E+00	.15726E+01	.17673E+01

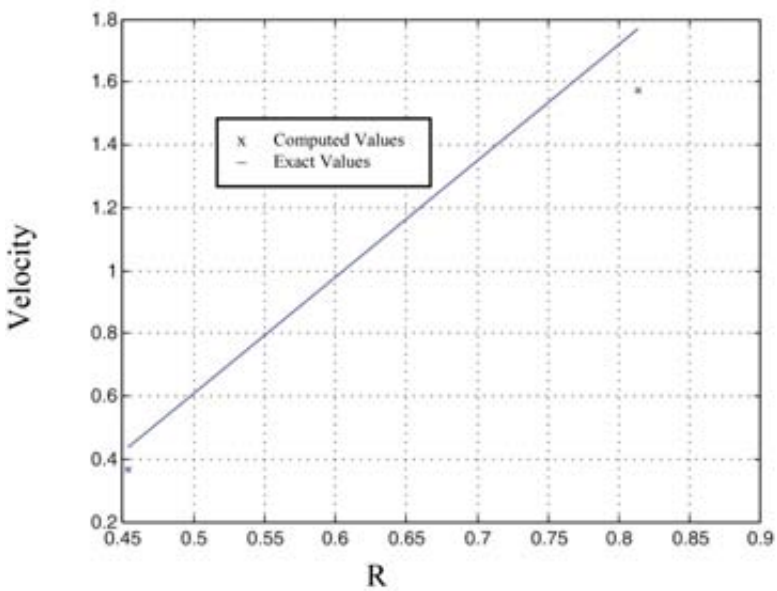

Figure 5 Comparison of computed and analytical velocity distributions over the surface of an oblate spheroid using 24 boundary elements with fineness ratio 10.

Table 3 Comparison of the computed velocities with exact velocity over the surface of an oblate spheroid with fineness ratio 2 using 96 boundary elements.

ELEMENT	XM	YM	ZM	$R = \sqrt{(YM)^2 + (ZM)^2}$	COMPUTED VELOCITY	EXACT VELOCITY
1	-.885E-01	-.934E+00	.177E+00	.95057E+00	.18636E+01	.24420E+01
2	-.261E+00	-.798E+00	.157E+00	.81353E+00	.12896E+01	.16013E+01
3	-.399E+00	-.522E+00	.157E+00	.54527E+00	.68456E+00	.84220E+00
4	-.467E+00	-.177E+00	.177E+00	.25022E+00	.25845E+00	.34596E+00
5	-.467E+00	.177E+00	.177E+00	.25022E+00	.25845E+00	.34596E+00
6	-.399E+00	.522E+00	.157E+00	.54527E+00	.68456E+00	.84220E+00
7	-.261E+00	.798E+00	.157E+00	.81353E+00	.12896E+01	.16013E+01
8	-.885E-01	.934E+00	.177E+00	.95057E+00	.18636E+01	.24420E+01
9	.885E-01	.934E+00	.177E+00	.95057E+00	.18636E+01	.24420E+01
10	.261E+00	.798E+00	.157E+00	.81353E+00	.12896E+01	.16013E+01
11	.399E+00	.522E+00	.157E+00	.54527E+00	.68456E+00	.84220E+00
12	.467E+00	.177E+00	.177E+00	.25022E+00	.25846E+00	.34596E+00
13	.467E+00	-.177E+00	.177E+00	.25022E+00	.25846E+00	.34596E+00
14	.399E+00	-.522E+00	.157E+00	.54527E+00	.68456E+00	.84220E+00
15	.261E+00	-.798E+00	.157E+00	.81353E+00	.12896E+01	.16013E+01
16	.885E-01	-.934E+00	.177E+00	.95057E+00	.18636E+01	.24420E+01
17	-.785E-01	-.798E+00	.522E+00	.95386E+00	.18585E+01	.24750E+01
18	-.235E+00	-.703E+00	.470E+00	.84578E+00	.14277E+01	.17433E+01
19	-.352E+00	-.470E+00	.470E+00	.66440E+00	.84484E+00	.11129E+01
20	-.399E+00	-.157E+00	.522E+00	.54527E+00	.68456E+00	.84220E+00
21	-.399E+00	.157E+00	.522E+00	.54527E+00	.68456E+00	.84220E+00
22	-.352E+00	.470E+00	.470E+00	.66440E+00	.84484E+00	.11129E+01
23	-.235E+00	.703E+00	.470E+00	.84578E+00	.14277E+01	.17433E+01
24	-.785E-01	.798E+00	.522E+00	.95386E+00	.18585E+01	.24750E+01
25	.785E-01	.798E+00	.522E+00	.95386E+00	.18585E+01	.24750E+01
26	.235E+00	.703E+00	.470E+00	.84578E+00	.14277E+01	.17433E+01
27	.352E+00	.470E+00	.470E+00	.66440E+00	.84484E+00	.11129E+01
28	.399E+00	.157E+00	.522E+00	.54527E+00	.68456E+00	.84220E+00
29	.399E+00	-.157E+00	.522E+00	.54527E+00	.68456E+00	.84220E+00
30	.352E+00	-.470E+00	.470E+00	.66440E+00	.84484E+00	.11129E+01
31	.235E+00	-.703E+00	.470E+00	.84578E+00	.14277E+01	.17433E+01
32	.785E-01	-.798E+00	.522E+00	.95386E+00	.18585E+01	.24750E+01
33	-.785E-01	-.522E+00	.798E+00	.95386E+00	.18585E+01	.24750E+01
34	-.235E+00	-.470E+00	.703E+00	.84578E+00	.14277E+01	.17433E+01
35	-.261E+00	-.157E+00	.798E+00	.81353E+00	.12896E+01	.16013E+01
36	-.261E+00	.157E+00	.798E+00	.81353E+00	.12896E+01	.16013E+01
37	-.235E+00	.470E+00	.703E+00	.84578E+00	.14277E+01	.17433E+01
38	-.785E-01	.522E+00	.798E+00	.95386E+00	.18585E+01	.24750E+01
39	.785E-01	.522E+00	.798E+00	.95386E+00	.18585E+01	.24750E+01
40	.235E+00	.470E+00	.703E+00	.84578E+00	.14277E+01	.17433E+01
41	.261E+00	.157E+00	.798E+00	.81353E+00	.12896E+01	.16013E+01
42	.261E+00	-.157E+00	.798E+00	.81353E+00	.12896E+01	.16013E+01
43	.235E+00	-.470E+00	.703E+00	.84578E+00	.14277E+01	.17433E+01
44	.785E-01	-.522E+00	.798E+00	.95386E+00	.18585E+01	.24750E+01
45	-.885E-01	-.177E+00	.934E+00	.95057E+00	.18636E+01	.24420E+01
46	-.885E-01	.177E+00	.934E+00	.95057E+00	.18636E+01	.24420E+01
47	.885E-01	.177E+00	.934E+00	.95057E+00	.18636E+01	.24420E+01
48	.885E-01	-.177E+00	.934E+00	.95057E+00	.18636E+01	.24420E+01

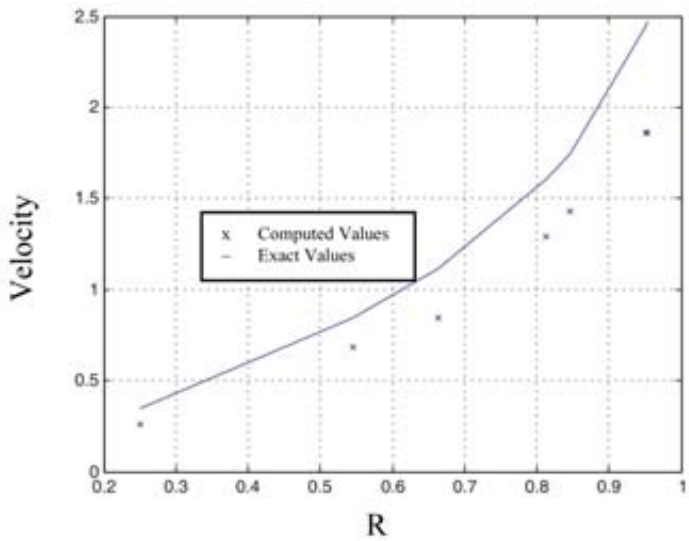

Figure 6 Comparison of computed and analytical velocity distributions over the surface of an oblate spheroid using 96 boundary elements with fineness ratio 2.

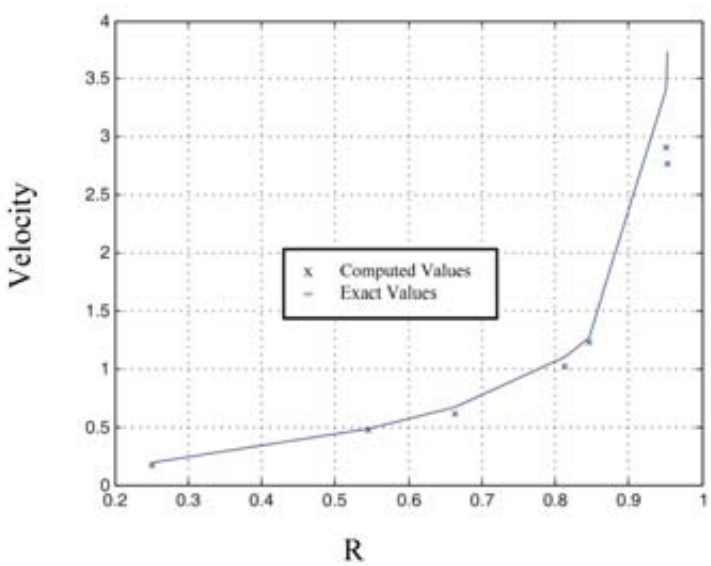

Figure 7 Comparison of computed and analytical velocity distributions over the surface of an oblate spheroid using 96 boundary elements with fineness ratio 10.

Table 4 Comparison of the computed velocities with exact velocity over the surface of a oblate spheroid with fineness ratio 10 using 96 boundary elements.

Element	XM	YM	ZM	$R = \sqrt{(YM)^2 + (ZM)^2}$	Computed velocity	Exact velocity
1	-.177E-01	-.934E+00	.177E+00	.95057E+00	.29112E+01	.34041E+01
2	-.522E-01	-.798E+00	.157E+00	.81353E+00	.10251E+01	.11072E+01
3	-.798E-01	-.522E+00	.157E+00	.54527E+00	.47407E+00	.49020E+00
4	-.934E-01	-.177E+00	.177E+00	.25022E+00	.17447E+00	.19264E+00
5	-.934E-01	.177E+00	.177E+00	.25022E+00	.17447E+00	.19264E+00
6	-.798E-01	.522E+00	.157E+00	.54527E+00	.47407E+00	.49020E+00
7	-.522E-01	.798E+00	.157E+00	.81353E+00	.10251E+01	.11072E+01
8	-.177E-01	.934E+00	.177E+00	.95057E+00	.29112E+01	.34041E+01
9	.177E-01	.934E+00	.177E+00	.95057E+00	.29112E+01	.34041E+01
10	.522E-01	.798E+00	.157E+00	.81353E+00	.10251E+01	.11072E+01
11	.798E-01	.522E+00	.157E+00	.54527E+00	.47407E+00	.49020E+00
12	.934E-01	.177E+00	.177E+00	.25022E+00	.17447E+00	.19264E+00
13	.934E-01	-.177E+00	.177E+00	.25022E+00	.17447E+00	.19264E+00
14	.798E-01	-.522E+00	.157E+00	.54527E+00	.47407E+00	.49020E+00
15	.522E-01	-.798E+00	.157E+00	.81353E+00	.10251E+01	.11072E+01
16	.177E-01	-.934E+00	.177E+00	.95057E+00	.29112E+01	.34041E+01
17	-.157E-01	-.798E+00	.522E+00	.95386E+00	.27699E+01	.37350E+01
18	-.470E-01	-.703E+00	.470E+00	.84578E+00	.12380E+01	.12744E+01
19	-.703E-01	-.470E+00	.470E+00	.66440E+00	.60931E+00	.67649E+00
20	-.798E-01	-.157E+00	.522E+00	.54527E+00	.47407E+00	.49020E+00
21	-.798E-01	.157E+00	.522E+00	.54527E+00	.47407E+00	.49020E+00
22	-.703E-01	.470E+00	.470E+00	.66440E+00	.60931E+00	.67649E+00
23	-.470E-01	.703E+00	.470E+00	.84578E+00	.12380E+01	.12744E+01
24	-.157E-01	.798E+00	.522E+00	.95386E+00	.27699E+01	.37350E+01
25	.157E-01	.798E+00	.522E+00	.95386E+00	.27699E+01	.37350E+01
26	.470E-01	.703E+00	.470E+00	.84578E+00	.12380E+01	.12744E+01
27	.703E-01	.470E+00	.470E+00	.66440E+00	.60932E+00	.67649E+00
28	.798E-01	.157E+00	.522E+00	.54527E+00	.47408E+00	.49020E+00
29	.798E-01	-.157E+00	.522E+00	.54527E+00	.47408E+00	.49020E+00
30	.703E-01	-.470E+00	.470E+00	.66440E+00	.60932E+00	.67649E+00
31	.470E-01	-.703E+00	.470E+00	.84578E+00	.12380E+01	.12744E+01
32	.157E-01	-.798E+00	.522E+00	.95386E+00	.27699E+01	.37350E+01
33	-.157E-01	-.522E+00	.798E+00	.95386E+00	.27699E+01	.37350E+01
34	-.470E-01	-.470E+00	.703E+00	.84578E+00	.12380E+01	.12744E+01
35	-.522E-01	-.157E+00	.798E+00	.81353E+00	.10251E+01	.11072E+01
36	-.522E-01	.157E+00	.798E+00	.81353E+00	.10251E+01	.11072E+01
37	-.470E-01	.470E+00	.703E+00	.84578E+00	.12380E+01	.12744E+01
38	-.157E-01	.522E+00	.798E+00	.95386E+00	.27698E+01	.37350E+01
39	.157E-01	.522E+00	.798E+00	.95386E+00	.27699E+01	.37350E+01
40	.470E-01	.470E+00	.703E+00	.84578E+00	.12380E+01	.12744E+01
41	.522E-01	.157E+00	.798E+00	.81353E+00	.10251E+01	.11072E+01
42	.522E-01	-.157E+00	.798E+00	.81353E+00	.10251E+01	.11072E+01
43	.470E-01	-.470E+00	.703E+00	.84578E+00	.12380E+01	.12744E+01
44	.157E-01	-.522E+00	.798E+00	.95386E+00	.27699E+01	.37350E+01
45	-.177E-01	-.177E+00	.934E+00	.95057E+00	.29112E+01	.34041E+01
46	-.177E-01	.177E+00	.934E+00	.95057E+00	.29112E+01	.34041E+01
47	.177E-01	.177E+00	.934E+00	.95057E+00	.29112E+01	.34041E+01
48	.177E-01	-.177E+00	.934E+00	.95057E+00	.29112E+01	.34041E+01

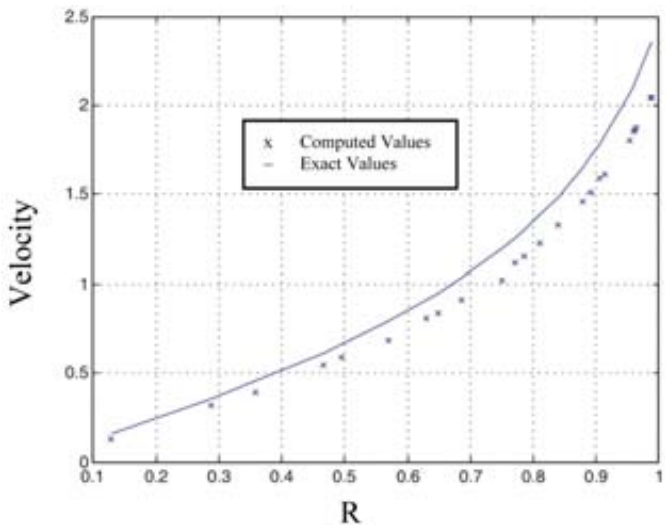

Figure 8 Comparison of computed and analytical velocity distributions over the surface of an oblate spheroid using 384 boundary elements with fineness ratio 2.

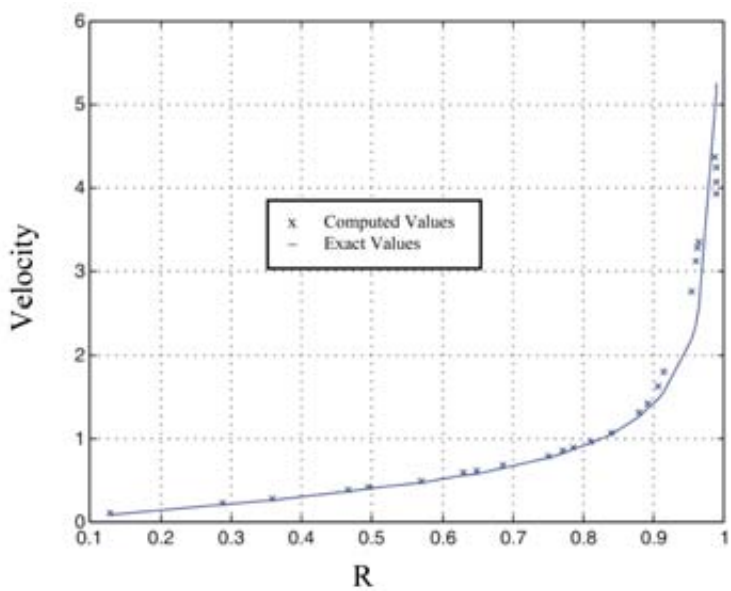

Figure 9 Comparison of computed and analytical velocity distributions over the Surface of an oblate spheroid using 384 boundary elements with fineness ratio 10.

ACKNOWLEDGEMENT

The authors are grateful to the University of Engineering & Technology, Lahore, Pakistan for financial support.

LITERATURE CITED

Hess, J.L. and A.M.O. Smith 1967. Calculation of potential flow about arbitrary bodies. **Progress in Aeronautical Sciences** 8: 1-158. Pergamon Press.

Hess, J.L. 1973. Higher order numerical solutions of the integral equation for the two-dimensional Neumann problem. **Computer Methods in Applied Mechanics and Engineering** 2: 1-15.

Morino, L., L.-T. Chen and E.O. Suciu. 1975. Steady and oscillatory subsonic and supersonic aerodynamics around complex configurations. **AIAA Journal** 13 (3): 368-374.

Brebbia, C.A. 1978. **The Boundary Element Method for Engineers.** Pentech Press. 46-86.

Brebbia, C.A. and S. Walker 1980. **Boundary Element Techniques in Engineering.** Newness-Butterworths. 25-60.

Shah, N.A. 2008. **Ideal Fluid Dynamics.** A–One Publishers, Lahore–Pakistan. 553-561

Mushtaq, M., N.A. Shah and G. Muhammad. 2009. Calculation of flow past a sphere in the vicinity of a ground using a direct Boundary Element Method. **Australian Journal of Basic and Applied Sciences** 3: 480-485.